Continuous DOPA synthesis from a single AAV: dosing and efficacy in models of Parkinson's disease.

Cederfjäll, Erik; Nilsson, Nathalie; Sahin, Gurdal; Chu, Yaping; Nikitidou, Elisabeth; Björklund, Tomas; Kordower, Jeffrey H; Kirik, Deniz

Link to publication

Continuous DOPA synthesis from a single AAV: dosing and efficacy in models of Parkinson's disease

Erik Cederfjäll[1], Nathalie Nilsson[1], Gurdal Sahin[1], Yaping Chu[2], Elisabeth Nikitidou[1], Tomas Björklund[1]*, Jeffrey H. Kordower[2] & Deniz Kirik[1]

[1]Brain Repair and Imaging in Neural Systems (B.R.A.I.N.S) Unit, Department of Experimental Medical Science, Lund University, Lund, Sweden, [2]Department of Neurological Sciences, Rush University Medical Center, Chicago, IL, USA.
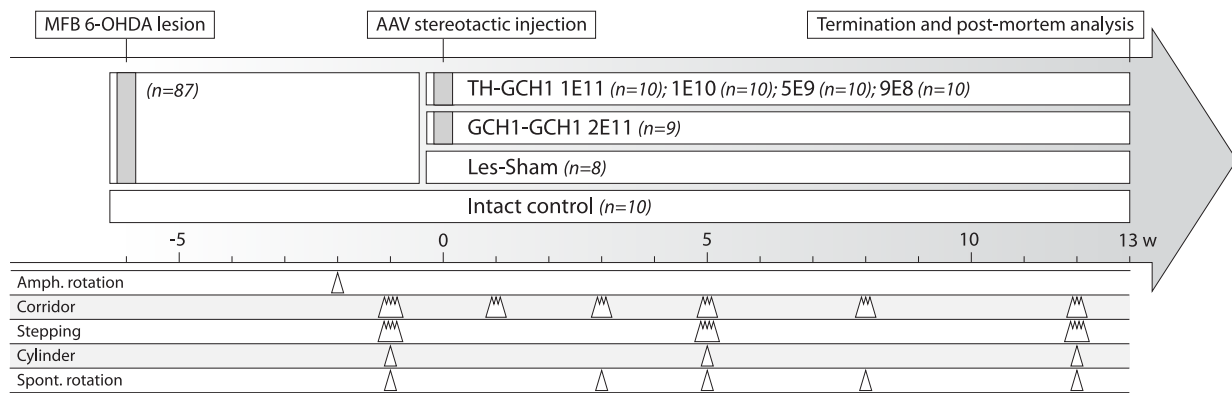
We used a single adeno-associated viral (AAV) vector co-expressing tyrosine hydroxylase (TH) and GTP cyclohydrolase 1 (GCH1) to investigate the relationship between vector dose, and the magnitude and rate of recovery in hemi-parkinsonian rats. Intrastriatal injections of >1E10 genomic copies (gc) of TH-GCH1 vector resulted in complete recovery in drug-naïve behavior tests. Lower vector dose gave partial to no functional improvement. Stereological quantification revealed no striatal NeuN+ cell loss in any of the groups, whereas a TH-GCH1 dose of >1E11 gc resulted in cell loss in globus pallidus. Thus, a TH-GCH1 dose of 1E10 gc gave complete recovery without causing neuronal loss. Safety and efficacy was also studied in non-human primates where the control vector resulted in co-expression of the transgenes in caudate-putamen. In the TH-GCH1 group, GCH1 expression was robust but TH was not detectable. Moreover, TH-GCH1 treatment did not result in functional improvement in non-human primates.

O ral administration of L-3,4-dihydroxyphenylalanine (L-DOPA) - immediate precursor to dopamine (DA) - provides potent symptomatic relief in Parkinson's disease (PD) patients. However, its long-term use results in development of disabling side effects such as wearing-off, on-off fluctuations and dyskinesias[1–3]. Continuous DA stimulation (achieved either by L-DOPA pumps or by DA agonist administration) results in reduction of dyskinesia and increases on-time during the day, possibly by reducing the fluctuation of the drug in the blood[4–7]. Replacement of the rate-limiting enzymes necessary for DA synthesis, namely tyrosine hydroxylase (TH) and GTP cyclohydrolase 1 (GCH1), is an alternative approach to achieve continuous production of DOPA in the striatum. Several pre-clinical studies, conducted by our group and others, supported the therapeutic robustness of this approach in rat models of PD[8–13]. In addition, other studies that included also the gene encoding the L-aromatic amino acid decarboxylase (AADC) – thus enabling transduced cells fully capable of producing DA – have shown efficacy in both rodents and non-human primates[14,15].

The studies cited above used separate adeno-associated virus (AAV) vectors for each transgene to drive the expression in the brain. We recently presented a new vector design where TH and GCH1 genes are co-expressed from a single AAV vector[16]. This dual-gene expression vector was very effective, as it provided robust recovery of the motor deficits in 6-hydroxydopamine (6-OHDA) injected rats where the ascending dopaminergic projections were completely lesioned. However, in a small cohort of animals, we found loss of NeuN positive neurons in the globus pallidus (GP) of TH-GCH1 treated animals. This finding was unexpected and concerning. Limited number of animals processed for histological analysis in this proof-of-concept work and the lack of a control vector treatment group prevented us from reaching definitive conclusions regarding the potential toxicity of the new TH-GCH1 vectors. We therefore designed the present work to address the following questions: (1) Is the neurotoxicity in GP dose-dependent; (2) Can we obtain functional recovery in rats in the absence of a frank neuronal loss in GP; (3) Are there any other measurable effects of over-dosing with this vector; and finally (4) What is the consequence of the expression in the non-human primate brain.

Results

TH-GCH1 dose-response analysis in the rat PD model. The relationship between total TH-GCH1 vector dose and the functional recovery in motor behavioral tests was assessed in rats following a complete unilateral lesion of the ascending dopaminergic projections from the ventral midbrain. All rats included in the study were assessed

Figure 1 | Experimental design for rodent study. Fifty-seven rats with complete lesions that fulfilled the criteria of > 6 net ipsiversive rotations over 90 min upon challenge with D-amphetamine (2.5 mg/kg) were included in the study. The animals were behaviorally characterized using corridor, stepping and cylinder tests and allocated to one of 6 groups based on their performance either to receive different doses of the TH-GCH1 vector (TH-GCH1:1E11, 1E10, 5E9 and 9E8 gc) or followed as one of two control groups (GCH1-GCH1:2E11 gc or Les-Sham). In addition, an intact control group (n = 10) was included in the study. Animals were followed over a 12-week period with behavioral tests to assess motor function as indicated in the time line. Thirteen weeks after AAV treatment, animals from each experimental group were sacrificed for either histology and stereology (n = 6) or biochemical analysis (n = 4, data not shown).
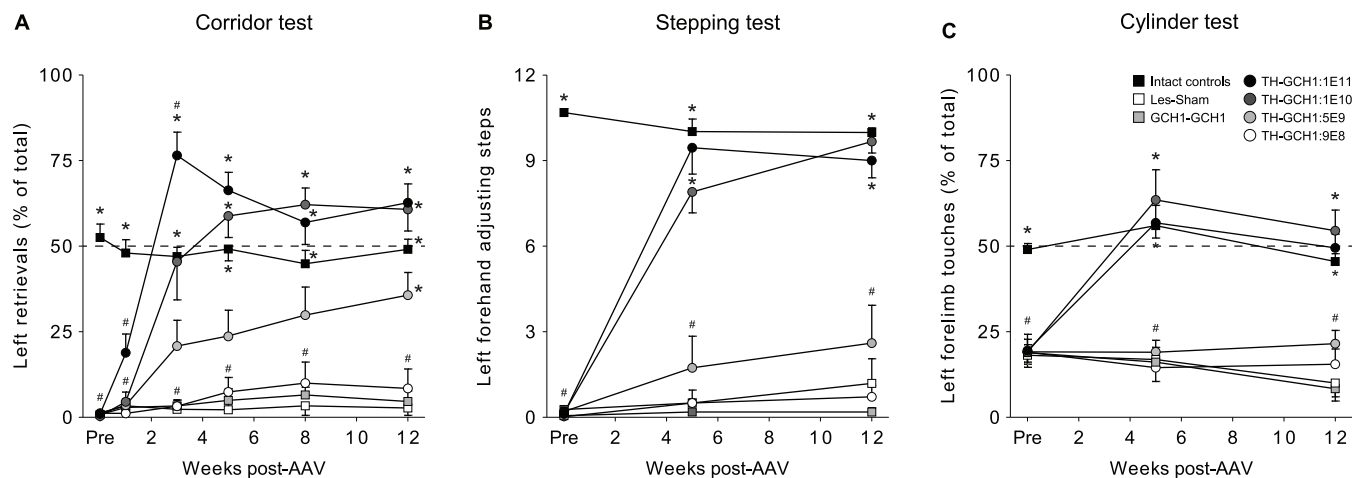
using three drug-naïve, simple, motor tasks starting 4 weeks after the 6-OHDA lesion surgery (Fig. 1). Behavioral assessment commenced with corridor test one week following AAV vector surgery, while the complete test battery was first applied at 5 weeks and longitudinal assessment continued for 3 months. Animals in the active treatment group (TH-GCH1) treated with the highest vector dose (1E11 gc; abbreviated TH-GCH1:1E11) already showed partial motor recovery in the corridor test on the contralateral side to the lesion at the one week time point (Fig. 2A). The magnitude of functional recovery in this group continued to increase and resulted in an overcompensation by 3 weeks, i.e., animals retrieved significantly more pellets on the affected side as compared with the intact side. This overcompensation was partly dampened at later time points. Although the affected paw use remained somewhat higher than intact rats, this difference was not significant at 5 weeks and beyond. This acute overcompensation was not seen in the TH-GCH1:1E10 group, but their long-term performance stabilized around the same level as the TH-GCH1:1E11 group. The animals in these two groups also showed complete recovery in the stepping (Fig. 2B) and cylinder (Fig. 2C) tests. Neither of these tests revealed any signs of overcompensation. The TH-GCH1:5E9 group showed partial recovery in the corridor test, which reached significant difference from the lesion controls (Les-Sham) group only at the 12-week time point but did not differ significantly in the stepping and cylinder tests at any time point tested here. The TH-GCH1:9E8 and the GCH1-GCH1 groups did not show any behavioral recovery. Taken together, these behavioral data suggest that at high doses, the biological activity of the TH and GCH1 enzymes expressed from the TH-GCH1 gene construct can be saturated, as a 10-fold dilution of the vector (from 1E11 to 1E10 gc) only slightly affected the time course of functional recovery, while the magnitude of long-term effects remained unchanged. Further lowering the dose, however, resulted in a significant reduction in extent of behavioral recovery and eventually to loss of efficacy at the lowest dose tested in this study.

Pattern and extent of transgene expression as a function of viral dose. Injection of the TH-GCH1 vector in the striatum (at two rostro-caudally separated injection tracts) resulted in dose-dependent transduction of the striatal cells, as seen with immunohistochemical detection of the TH (Fig. 3) or the GCH1 enzymes (Fig. 4). Although no behavioral recovery was observed in the TH-GCH1:9E8 group, the expression of transgenic TH protein was visible in both striatum and GP (Fig. 3C), and this staining was not present in the Les-Sham group

(Fig. 3B). In the TH-GCH1:5E9 group, not only the volume of transduction in the targeted tissue was increased but also the transduction became detectable in deep layers of the overlying cortical region (Fig. 3D). Delivery of higher doses (1E10 gc, Fig. 3E and 1E11 gc, Fig. 3F) resulted in wider TH staining covering almost the entire striatum and GP with an accompanying transduction of ventral aspects of the overlying cortex. Sections stained for human transgenic GCH1 enzyme (Fig. 4) showed a similar spread of the transgene in the striatum, GP and cortex in the TH-GCH1 injected animals (Fig. 4B–E) and the GCH1-GCH1 control group (Fig. 4F).

Effect of transduction on the integrity of pallidal neurons. In the low dose TH-GCH1 groups, transduction in the striatum was small, but was associated with transgene immunoreactivity in both terminals of striato-pallidal neurons and single neurons in GP (Fig. 5). In the high dose groups, on the other hand, the spread and amount of the vector was greater and caused a larger transduction of the GP neurons. Importantly, the organization of the pallidal neurons and their dendritic processes appeared to be affected. In order to better evaluate the possible adverse effects of transgene expression in the GP, we carried out immunohistochemical analysis with additional markers including NeuN and Nissl stain using cresyl violet to assess the integrity of neuronal profiles in this region, as well as markers for microglia, Iba1 and ED1, to assess presence of any inflammatory response in the tissue.

In the TH-GCH1 treated animals, we observed a dose-related reduction in NeuN positive neurons in the GP (as illustrated in Fig. 5, row 2). The control vector expressing only the GCH1 gene did not appear to induce any loss of NeuN positive cells despite the fact that its titer was at the highest level tested with the TH-GCH1 vectors. Nissl-stained sections from adjacent sections supported the view that some of the GP neurons in the high dose TH-GCH1 injected animals might have been lost after the transduction. There was, however, no sign of hyper-cellularity of perivascular cuffing suggesting that no infiltration of blood born immune cells was occurring at the time of sacrifice. Inspection of specimens stained for Iba1, which is a marker for microglial cells in the brain, showed a corresponding increase in the intensity of Iba1 labeling where the cell loss was seen (Fig. 5, row 4). Increased intensity of labeling as well as altered microglial morphologies was most profound in the three high doses of the TH-GCH1 treated animals, while the lowest dose group or the GCH1-only control vector treated animals had minimal or no alteration as compared with the lesion control group or the intact

Figure 2 | Recovery of motor function in drug-naive behavior tests over the 12-week follow up after AAV treatment. Due to the ease in longitudinal assessments, the corridor test (A) was administered at several time points, which revealed an early partial recovery in the TH-GCH1:1E11 group at 1 week, a transient overcompensation (strong contralateral bias) at 3 weeks and a stable response with slight bias in left retrievals at 5 weeks and onwards. Animals in the TH-GCH1:1E10 group displayed a similar behavior, however, at a slower rate and without the overcompensation at 3 weeks post-AAV. The TH-GCH1:5E9 group showed only partial recovery but were significantly different from Les-Sham at the 12 week time point. Animals receiving the TH-GCH1:9E8 and GCH1-GCH1:2E11 did not show any recovery compared with Les-Sham. Behavioral recovery in the stepping (B) and cylinder (C) tests were comparable in the 1E11 and 1E10 groups, while the response in the 5E9 group was less pronounced or not detectable, respectively. Statistics: Repeated measures ANOVA (A) Time $F_{(3,20)} = 65.85$ $p < 0.001$; Time $\times$ Group $F_{(3,20)} = 16.64$ $p < 0.001$; (B) Time $F_{(2,9)} = 129.05$ $p < 0.001$; Time $\times$ Group $F_{(2,9)} = 39.26$ $p < 0.001$; (C) Time $F_{(2,12)} = 73.82$ $p < 0.001$; Time $\times$ Group $F_{(2,12)} = 43.86$ $p < 0.001$; One-way ANOVA at each time point followed by *post hoc* comparison with Tukey's HSD when Levene's test was significant ($p < 0.05$) otherwise by Dunnett's T3 test. * = different from Les-Sham $p < 0.05$, # = different from intact controls $p < 0.05$. Error bars represent mean SEM.

brain. Activation of microglia in the GP where cell loss occurred was confirmed by positive staining for the ED1 marker, which labels only activated, macrophagic microglia (Fig. 5, row 5).
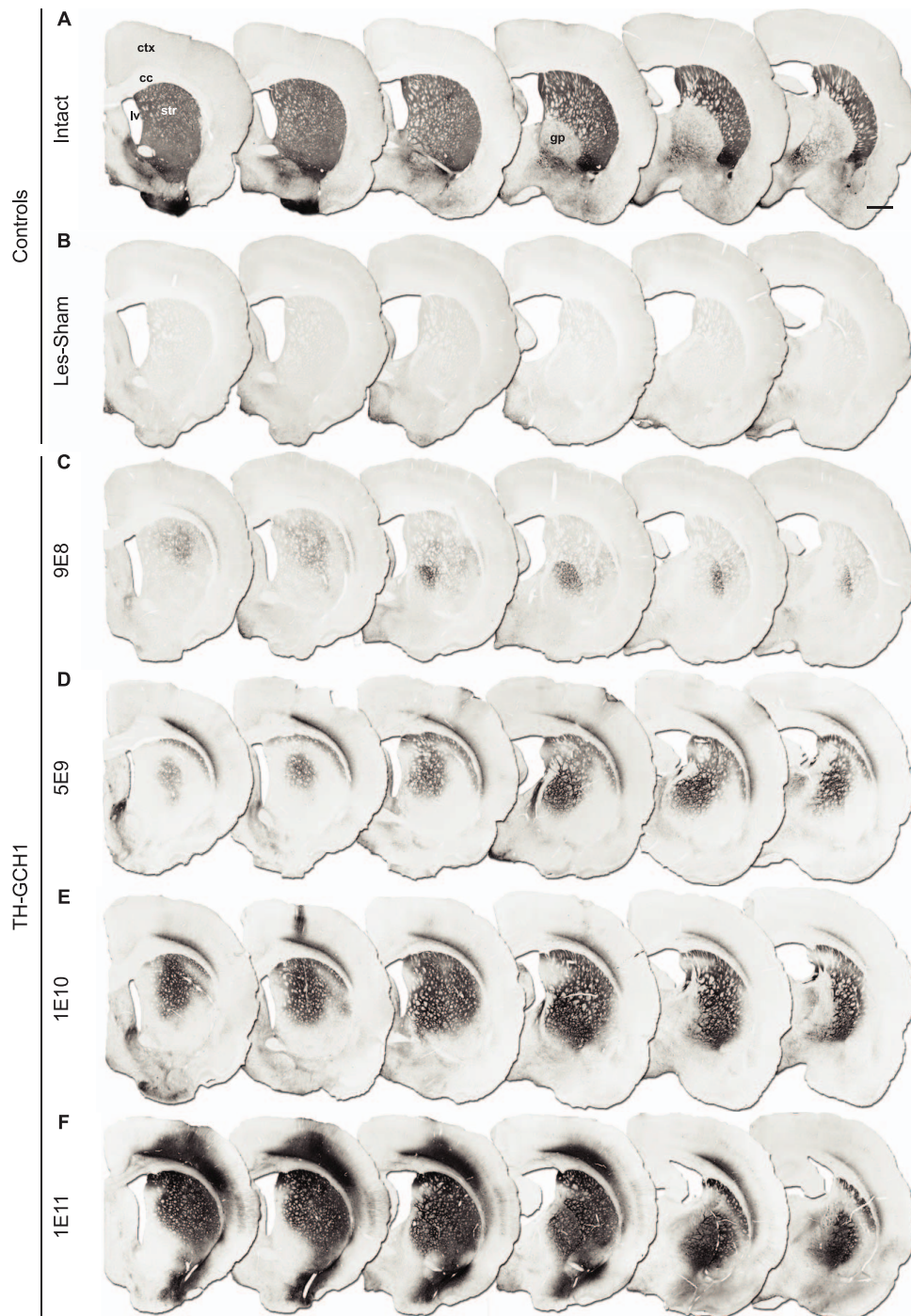
Based on the observations above, we performed stereological quantification of NeuN positive cells to investigate the magnitude of cell loss that occurred in the striatum (intended target site) or the GP (adjacent structure transduced by vector spread beyond the target region). In addition to the material generated in this experiment, we processed histological specimens we have generated in the previous proof-of-principle study[16] for NeuN staining and stereological quantification. In that study the same TH-GCH1 vector construct was used at 2E12 gc dose but this analysis was not performed, however the results were relevant in the present context. We found that none of the vector doses in the TH-GCH1 or the GCH1-GCH1 groups resulted in a measurable NeuN positive cell loss in the striatum (Fig. 6A). However, there was a significant loss of NeuN positive cells in the GP of animals treated with the TH-GCH1 at high doses (1E11 and 2E12 gc) (Fig. 6B). The GCH1-GCH1 vector (2E11 gc) did not result in NeuN positive cell loss in the GP, suggesting that the cell loss was unlikely to be due to the vector dose per se, rather the composition of the transgenes expressed and/or the biological effect associated with DOPA synthesis. Analysis of the distribution of NeuN positive cells in the rostrocaudal axis of GP in the different experimental groups illustrated that the loss was predominantly in the rostral GP, while most caudal aspects appeared less affected (Fig. 6C).

Expression of the TH-GCH1 vector in the non-human primate brain. Next we studied the effect of TH-GCH1 expression in the 1-methyl-4-phenyl-1,2,3,6-tetrahydropyridine (MPTP) treated non-human primate brain. Six *cynomolgus macaques* with stable MPTP-induced motor impairment received intracerebral injections (two injections in caudate at 5 μl and three injections in putamen at 10 μl) of either the TH-GCH1 vector (n = 3) or a control vector expressing GFP-GCH1 (n = 3), at a total dose of 2.6E12 gc. Specimens processed for GCH1 immunohistochemistry showed

that the expression of this transgene was clearly detectable. GCH1 positive cells were observed in both the putamen and caudate nucleus. Anterograde transport of the vector/transgene was also seen in the internal and external segments of GP (Fig. 7A–B). Transgenic human TH could not be detected with immunohistochemistry, in contrast to residual endogenous TH expression in the monkey. Notably, the same antibody was used in rodent where both transgenic TH and rodent endogenous TH could be detected. Quantification of GCH1 positive cells in vector-treated animals showed that 760,800 ± 138,901 and 406,100 ± 129,997 cells were transduced in the putamen and caudate nucleus in the TH-GCH1 group, and 277,800 ± 127,835 and 169,812 ± 121,239 cells in the GFP-GCH1 group, respectively (Fig. 7C). Based on our stereological estimation of the total NeuN positive cells in the intact animals (9,824,000 ± 339,741 and 8,089,000 ± 480,337 cells in putamen and caudate nucleus) in this study, the above numbers correspond to 2.8 ± 0.4% and 7.7 ± 0.4% of the total cell numbers in the putamen and 2.1 ± 0.3% and 5.0 ± 0.3% in the caudate nucleus. Of note, NeuN stained specimens from the vector treated animals suggested that there was not a frank cell loss associated with vector treatment, in either the GFP-GCH1 or TH-GCH1 group (Fig. 7E–F). Since the transgenes are driven with a neuronal promoter from a single AAV vector, we expected that the transgene expression would have an overlapping expression pattern with NeuN. This was evidenced by triple immunofluorescence labeling with NeuN, GFP and GCH1 and co-localization using confocal analysis (Fig. 7G).

Extracellular monoamine levels were measured in all animals with microdialysis, however, only cases where correct probe placement could be confirmed were included (TH-GCH1 n = 4, GFP-GCH1 n = 4, Intact n = 2). After collection of the five samples under baseline conditions, an AADC inhibitor was injected (NSD-1015, 100 mg/kg, iv) to study TH enzyme function and efficiency in vivo by assessment of DOPA accumulation in the putamen. Under these experimental conditions there was a robust increase in the DOPA levels in the intact putamen (Fig. 8A). This was accompanied with a reduction of the AADC catalyzed conversion product, DA (Fig. 8B) and its
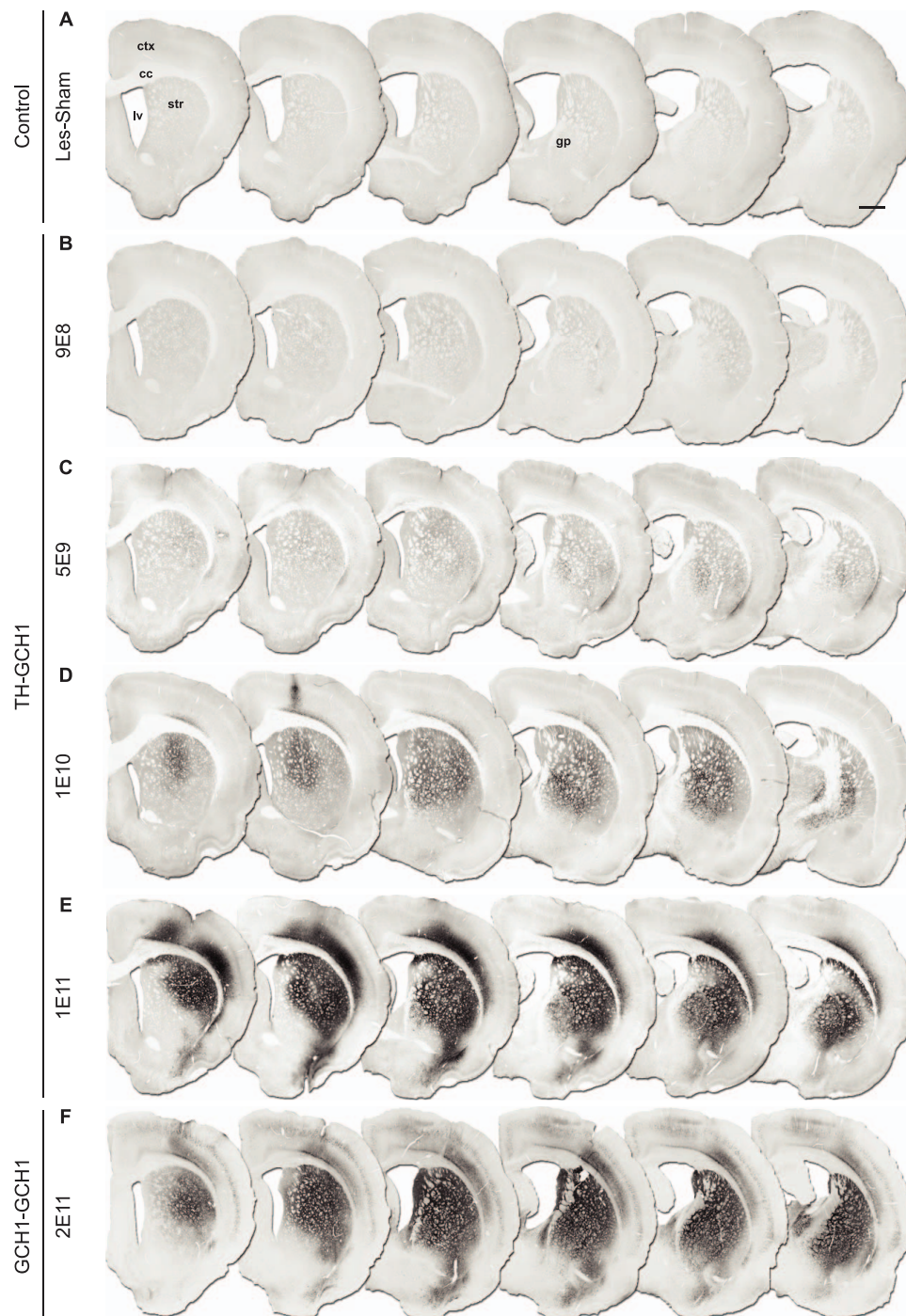
Figure 3 | **Dose-dependent increase in TH transgene expression.** Intrastriatal injections of an AAV vector expressing TH and GCH1 at 9E8 gc results in a small number of TH positive neuronal profiles in the striatum and in globus pallidus (C). Increasing the vector dose to 5E9 gc (D) resulted in larger transduction area in the striatum and further spread to globus pallidus and cortex. Injection of 1E10 and 1E11 gc gave more widespread transduction not only in the striatum but also more extensive expression in the globus pallidus and overlying cortex (E,F). ctx = cortex, cc = corpus callosum, gc = genomic copies, gp = globus pallidus, lv = lateral ventricle, str = striatum. Scale bar in a represent 0.2 mm in all panels.

metabolite 3,4-dihydroxyphenylacetic acid (DOPAC) (Fig. 8C). As expected, DOPA accumulation was severely blunted in the MPTP treated animals that received the GFP-GCH1 control vector. These animals had very low DA, DOPAC and homovanillic acid (HVA) levels in the baseline, thus no alterations were detectable after NSD-1015 treatment. In the TH-GCH1 treated monkeys, we expected to see a recovery of DOPA synthesis capacity (as would be seen after NSD-1015), and normalization of DOPAC and HVA levels in the baseline, as well as increase in extracellular DA levels. However,

TH-GCH1 treatment had no robust effects on these parameters (all tested effects were statistically insignificant) (Fig. 8A–D).

Motor assessment of the MPTP treated monkeys was carried out longitudinally with the non-human primate equivalent of the clinical rating scale (CRS). MPTP administration (employing a chronic systemic dosing regimen) caused a gradual evolution of severe motor disability in the animals that was stabilized at 6–7 months after the initial dosing. At 12 months after the initial dose (5 months after the stabilization of the motor deficits), AAV vectors were injected and

Figure 4 | Dose-dependent increase in GCH1 transgene expression. Note that the antibody used here does not cross react with the rodent protein and thus only shows the transgenic human GCH1 expressed from the AAV vector. Intrastriatal injections of 9E8 gc TH-GCH1 vector (B) resulted in very few GCH1 positive neurons in the striatum and globus pallidus, whereas the transduction efficiency increased with vector doses of 5E9 gc (C), 1E10 (D) and 1E11 gc (E). The two high doses resulted in complete coverage of striatum and globus pallidus (D,E). The transduction spread was similar in the GCH1-GCH1 control vector group (E,F). ctx = cortex, cc = corpus callosum, gc = genomic copies, gp = globus pallidus, lv = lateral ventricle, str = striatum. Scale bar in a represent 0.2 mm in all panels.

animals followed for 6 months before the microdialysis experiment and killing. In line with the observations above, none of the animals showed any sign of recovery in motor performance (Fig. 8E). In addition, the animals were challenged with peripheral L-DOPA in increasing concentration (10, 20 and 40 mg/kg) over 9 consecutive days, both pre- and post-AAV treatment. Quantification of the motor response in this test suggested that the animals were not responsive to L-DOPA treatment prior to AAV and the vector treatment did not change this result (Fig. 8F).

Discussion

Delivery of 1E10 gc TH-GCH1 to DA depleted rats resulted in complete recovery in all three spontaneous behavioral tests used in this study, suggesting that robust effects can be obtained in rodents using

Figure 5 | High magnification images of neurons in the globus pallidus (GP). Transgene immunoreactivity (row 1, TH staining depicted in all panels except GCH1-GCH1 which is a GCH1 staining) was present in GP in all vector-treated animals filling cell bodies, dendritic processes and axon terminals. Loss of NeuN positive cells in GP was seen in animals injected with 1E11 gc of the TH-GCH1 vector (row 2, far right) but also to a lesser extent in the 1E10 group. Nissl stained specimens from adjacent sections confirmed loss of neurons (row 3)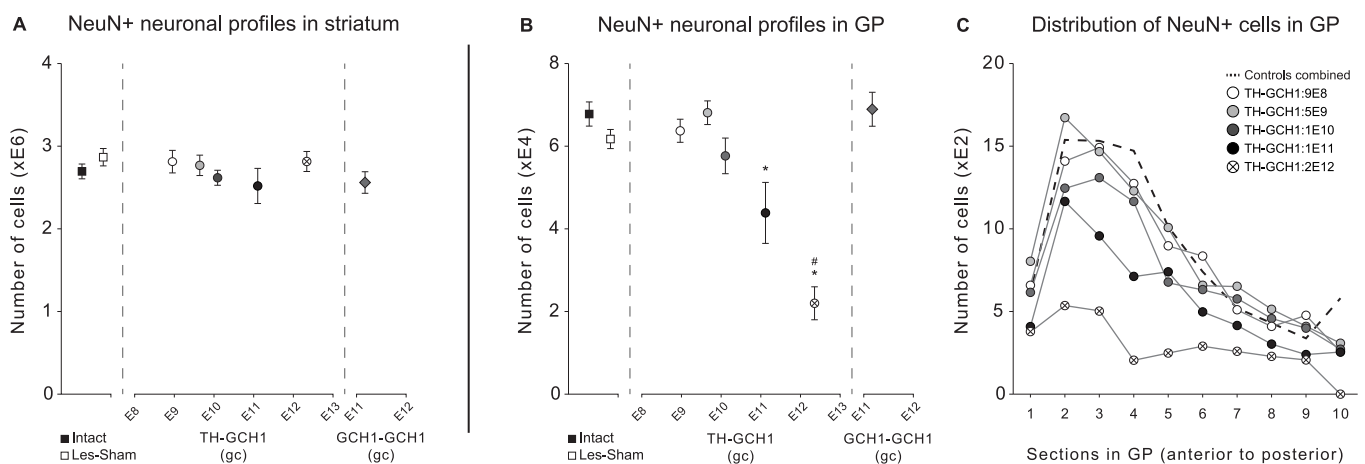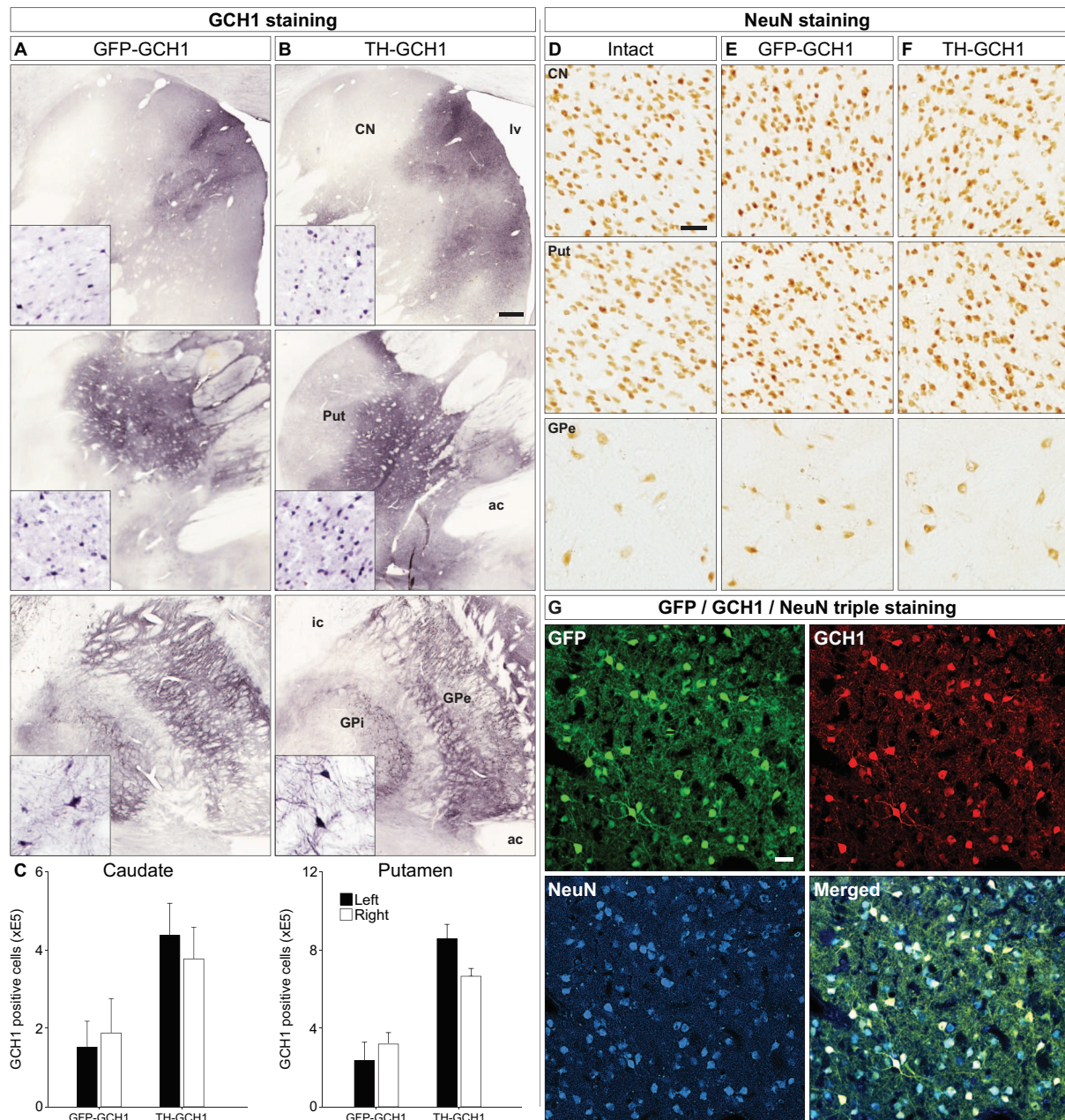. In the same region, there was an increase in the microglial marker Iba1 (row 4) seen as a dose-dependent increase in arborized reactive cells. ED1 (equivalent to human CD68) immunoreactivity indicated presence of macrophages. Scale bar in top left panel represent 0.2 mm in all panels.

Figure 6 | Quantification of NeuN-positive neurons with stereological analysis in both striatum (A) and globus pallidus (B). Vector-treatment did not result in any decrease in cell number in the striatum, regardless of dose (A). However, quantification of NeuN positive cells in globus pallidus revealed a significant decrease in animals treated with TH-GCH1 vector dose of 1E11 gc or higher. Inspection of the distribution of NeuN positive cell counts in the globus pallidus (C) suggested that the decrease was primarily in the anterior part of the structure. The TH-GCH1 vector at doses below 1E10 or GCH1-GCH1 vector treatments showed no apparent loss of either striatal or pallidal NeuN positive cells. Statistics: One way ANOVA: (A) $F(7,36) = 0.88$, (B) $F(7,36) = 12.18$ $p < 0.001$, followed by Tukey's HSD *post hoc* since Levene's test was not significant. * = different from Les-Sham $p < 0.001$, # = different from intact controls $p < 0.001$. Error bars represent mean SEM.
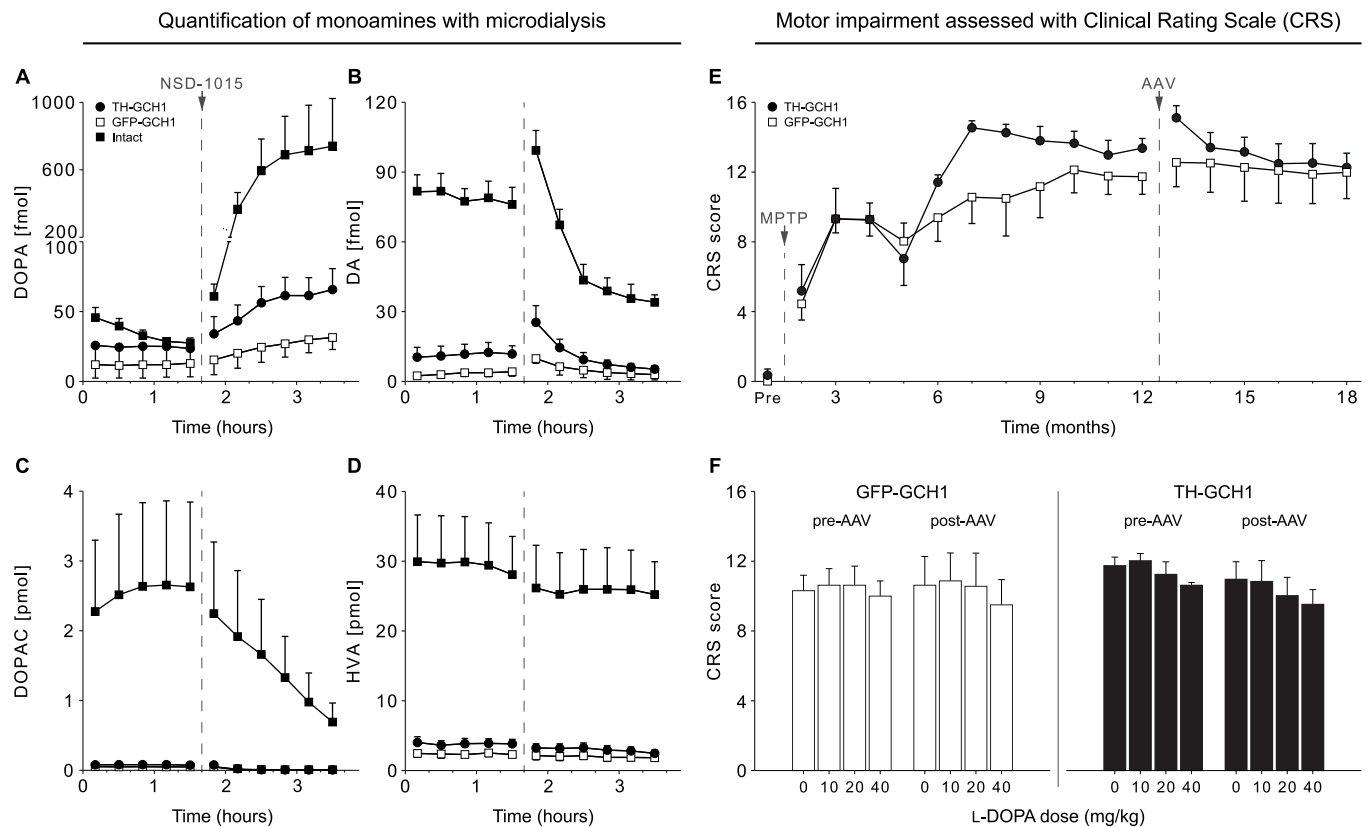
Figure 7 | Transgene expression in MPTP-treated monkeys. Transgene expression from both AAV vectors encoding GFP-GCH1 (A) and TH-GCH1 (B) were visualized with the GCH1 antibody, which showed GCH1 immunoreactivity in the putamen (Put, row 1), caudate nucleus (CN, row 2) and globus pallidus (GP, row 3). Interestingly, both the external and internal segment of GP had GCH1 immunoreactive cells and projections (insets). Stereological quantification of GCH1 positive neurons was performed in both putamen and caudate nucleus bilaterally (C). NeuN stainings were performed in adjacent sections and are shown from Put, CN and GPe (E-F). Co-expression of GFP and GCH1 in the transduced neurons was confirmed with confocal microscopy (G). Whereas the GCH1 staining was robust, the expression of the TH transgene could not be confirmed in the TH-GCH1 injected monkeys. ac = anterior commissure, CN = caudate nucleus, GPi/GPe = globus pallidus internal/external segment, lv = lateral ventricle, Put = putamen. Scale bar in (B) represent 0.5 mm and (D) and (G) represents 50 μm. GCH1 insets in (A–B) have the same magnification as (D). Cell counts in (C) represent mean SEM.

this vector. Further increasing the dose to 1E11 gc did not yield any additional behavioral benefits except a more rapid response, that was detectable with the corridor test already one week after vector-injection. The higher dose was however also associated with an over-compensation or hyper-focus of the ipsilateral space, which resulted in some animals only retrieving pellets from the right side (ipsilateral to the lesion) and neglecting the contralateral intact side in the corridor test. The overcompensation effect was transient as it was most prominent at 3 weeks post-AAV, declined at 5 weeks and gradually plateaued at a level not different from intact controls. We have not observed the overcompensation response using this approach in previous studies, possibly due to later initiation of behavioral testing. Lowering the dose of TH-GCH1 to 5E9 gc resulted in a partial recovery in the corridor test that was statistically different from Les-Sham only at the 12-week time point, while the lowest dose remained ineffective.

The stereological quantification of NeuN positive cells revealed that the TH-GCH1 vector injected at a dose of 1E11 gc resulted in a measurable reduction in NeuN positive neurons in GP compared with intact and lesion controls. Nissl stained sections in adjacent

7

Quantification of monoamines with microdialysis

Motor impairment assessed with Clinical Rating Scale (CRS)

Figure 8 | Six MPTP lesioned stably parkinsonian *cynomolgus macaques* received bilateral AAV injections in the caudate-putamen with either TH-GCH1 (n = 3) or GFP-GCH1 (n = 3) and were followed for 6 months. After the last assessment point at 18 months, microdialysis was performed on all vector-treated animals and two intact controls by placing bilateral probes in the putamen (A–D). In the analysis, we only included cases where probe placement could be histologically confirmed (TH-GCH1 n = 4, GFP-GCH1 n = 4, Intact n = 2). After one hour equilibration, five baseline samples á 20 minutes were collected. Baseline levels of DA was decreased by 96% in GFP-GCH1 when compared with intact controls in response to the MPTP lesions (B). During sampling of the fifth baseline sample, all animals received an iv injection of the central AADC inhibitor NSD-1015 (100 mg/kg in saline). Inhibition of AADC resulted in an accumulation of DOPA in intact animals (A), whereas this increase was blunted in the vector control group and only marginally higher in the TH-GCH1 treated monkeys. Simultaneously, DA (B) and its immediate metabolite DOPAC (C) were markedly reduced in intact animals. This could not be detected in the vector-treated animals. HVA levels (D) remained at a constant level throughout the experiment. The animals were assessed behaviorally using the non-human primate equivalent of the clinical rating scale (CRS), both pre- and post-AAV treatment longitudinally under baseline conditions (E) or following L-DOPA administration (F) (10, 20 or 40 mg/kg dose). Error bars represent mean SEM.

series confirmed loss of cell bodies consistent with neuronal profiles supporting the concept that frank cell loss was observed and the changes seen were not the result of a immunohistochemical down-regulation of NeuN. The same TH-GCH1 vector used in the previous study (at 2E12 gc dose and processed at 12 weeks post-AAV injection) also showed a robust cell loss[16]. Notably, the GCH1-GCH1 vector control group, matched in titer to the TH-GCH1:1E11 group, did not show any evidence of cell loss. This suggests that the loss of NeuN positive neurons in the GP was not due to the AAV vector itself or BH4 synthesis per se, but more likely associated with DOPA production and its downstream effects on these cells. Interestingly, high DOPA levels can clearly be toxic *in vitro*, and has been proposed to be toxic *in vivo*, but this is one of the few data sets that reveal such toxicity in animal models[17–19]. The three other TH-GCH1 vector doses tested here did not cause significant cell loss in GP when compared with lesion and intact controls. Importantly, no vector-treatment group, including the TH-GCH1 group from the previous study, had any loss of NeuN positive neurons in the striatum. It appears, therefore, that the rat pallidal neurons might be more sensitive to transduction with TH-GCH1 genes as compared with the striatal neurons. In addition to GP, we noted a robust transduction in deep layers of the overlying cortex most prominently in the TH-GCH1:1E11 group. Spread to

cortical areas was present in much less extent in the TH-GCH1:1E10 group. Taken together, 1E10 gc of TH-GCH1 resulted in complete behavioral recovery in complete 6-OHDA lesioned rats, without causing significant toxicity to GP or striatal neurons. This suggests that the dose of the TH-GCH1 vector can be adjusted to retain efficacy without compromising safety. However, the therapeutic window is narrow in the rat model, as a 3-fold dilution of the vector from effective non-toxic dose resulted in incomplete behavioral recovery. It is not clear, at this point, if the therapeutic window could be different in vectors utilizing different promoters, expressing the two enzymes separately, or if the enhanced TH-expression achieved through the use of the woodchuck hepatitis virus post-transcriptional regulatory element (WPRE) might be playing a critical role in observed toxicity. Additionally, it remains possible that the therapeutic window might be different using other model systems such as those based on alpha synuclein toxicity or a partial 6-OHDA denervation model, mimicking earlier stages of the disease with a larger remaining DA storage capacity. In a recent study by Ciesielska and colleagues transduction of antigen presenting cells (APC) resulted in neurotoxicity with an AAV9 vector expressing GFP or AADC under a CMV promoter[20]. Although contribution from APC on cell loss in the present study cannot be ruled, differences in serotype tropism and the use of the neuron
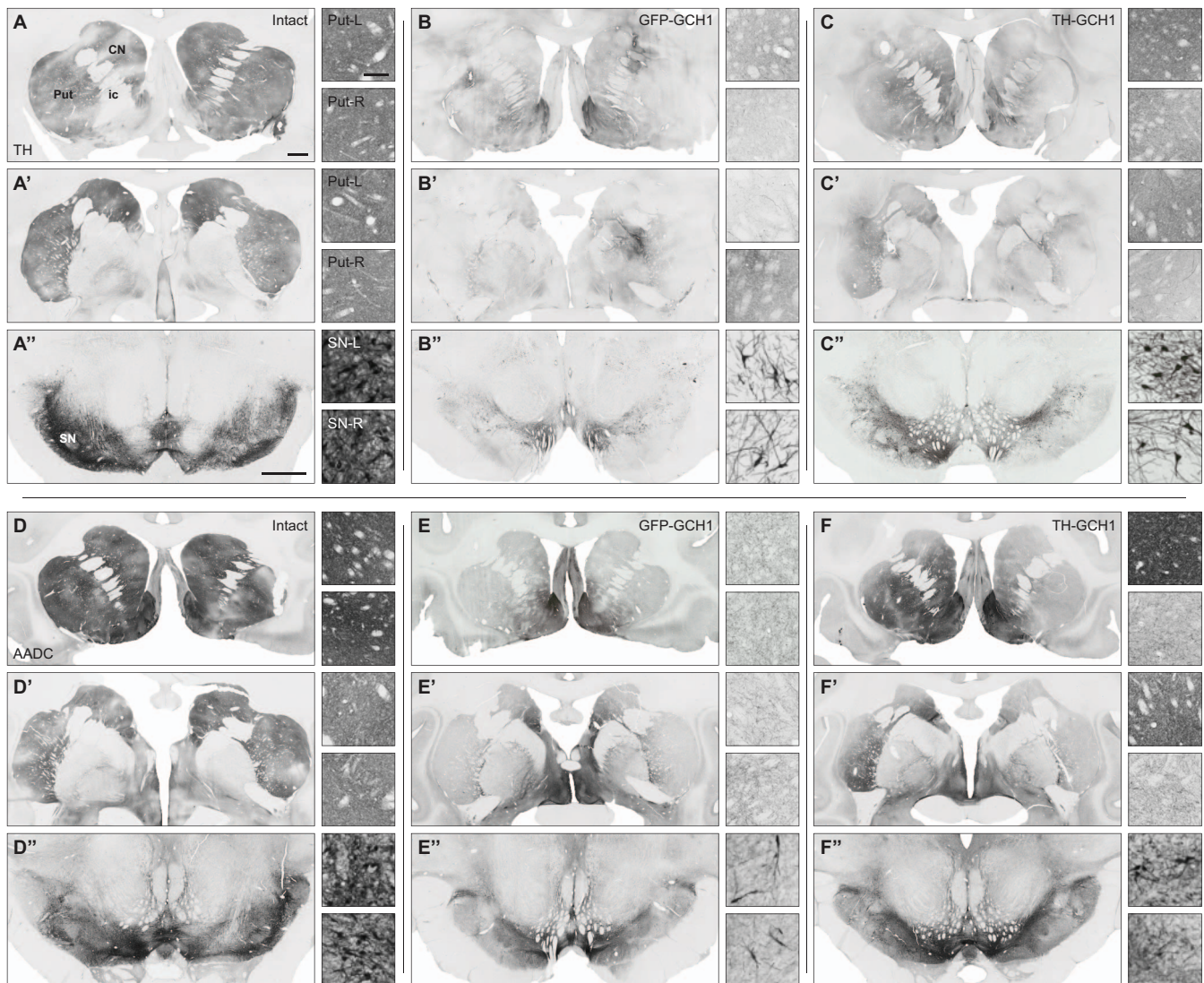
specific synapsin-1 promoter instead of the ubiquitous expressing CMV promoter, would argue against. Further studies will be required to address these questions.

Next, we tested the effect of TH-GCH1 vector in a small cohort of MPTP-lesioned non-human primates. In three monkeys that received the TH-GCH1 vector, the treatment did not result in any beneficial effect during the 6-month assessment period. Unlike what was observed in rodents, we did not observe any increases in DOPA, DA or DA metabolites as assessed by microdialysis. There was also no accumulation of DOPA after inhibition of the AADC with NSD-1015 in the two vector-treated groups. In studies by Bankiewicz and colleagues, AADC activity was shown to be decreased in the MPTP monkey model but the animals were still L-DOPA responsive[21,22]. This suggests that AADC activity is not a limiting factor in this model. The monkeys used in the present study however, did not respond to peripheral L-DOPA, which is required for this gene therapy approach. Histological analysis of the brain tissue revealed extensive decrease in TH and AADC positive cells in the caudate putamen on both sides in four of the six monkeys (Fig. 9B,E). The remaining two MPTP lesioned monkeys had spared innervation on the contralateral side to the intracarotid artery injection (Fig. 9C,F). This overall extensive denervation could explain the lack of L-DOPA response.

Additionally, no functional improvement was observed using a validated CRS or an objective hand reach task (data not shown). Surprisingly, post-mortem assessments of transgene expression demonstrated robust expression of GCH1, GFP, but not TH. This again is in contrast to what we found in rodents using the same vector preparation where robust expression of both TH and GCH1 was observed. This did not appear to be related to vector construction, since the expression of the GCH1 and GFP transgenes was readily detected in the monkey brain. However, we did find that the GCH1

Figure 9 | Residual TH and AADC expression in the MPTP lesioned monkey brain. Pre-commissural and post-commissural caudate-putamen, and the substantia nigra stained for TH (A–C) or AADC (D–F) from the intact (A,D), GFP-GCH1 (B,E) and TH-GCH1 (C,F) groups. Insets are high-power images from the left and right hemisphere respectively. MPTP was administered via the right intracarotid artery and by systemic doses until stable parkinsonian impairments were obtained, which varied between the individual monkeys. Two out of six monkeys had spared dopaminergic innervation on the contralateral side to the intracarotid injections (as shown in C), whereas the remaining four were severely lesioned in both hemispheres (as shown in B,E). Since the number of TH and AADC positive cells in ventral tier of substantia nigra in B and C was greatly reduced, the high power insets are from the dorsal tier. TH expression observed in B and C was not vector-derived. CN = caudate nucleus, ic = internal capsule, Put = putamen, SN = substantia nigra. Scale bars in A (that also applies to A′) and A′′ represent 2 mm. Scale bar in the high-power inset Put-L represent 0.5 mm, whereas it represents 0.25 mm in SN-L and SN-R.

positive cell counts in the putamen and caudate nucleus in both groups studied here were lower than what we found in a previous study[23]. In the previous work, the quantification of GFP positive cells using the same AAV5 serotype, but with 15-fold lower gc injected, resulted in approximately 500,000 transduced cells, as compared with 760,000 and 280,000 cells in this study with TH-GCH1 and GFP-GCH1 respectively. A controlled study comparing the efficacy of the CBA promoters used in the Dodiya (2010) paper and the synapsin-1 (Syn1) promoter (as used here) in the monkey striatum would be very informative in deciding which one of these two promoters are more likely to work better in the human brain.

The reason for the lack of transgenic TH expression by histology and lack of DOPA and dopamine production by microdialysis remains unclear at this time. However, this problem requires a solution prior to the initiation of clinical trials utilizing this approach.

In summary, gene therapy with TH and GCH1 provides a dose-dependent functional recovery in unilateral 6-OHDA lesioned rats that is mediated by enhanced DOPA production. Work to widen the therapeutic window would benefit the therapeutic pipeline for this approach. Finally, an unexpected dysregulation of transgene expression using the same vectors was observed in parkinsonian monkeys in which GCH1, but not TH, was observed following treatment. This issue should be resolved prior to proceeding towards clinical trials.

Methods

Subjects. For the rodent studies, eighty-seven female Sprague-Dawley rats weighing 225–250 g were purchased from Charles River (Schweinfurt, Germany) and housed 2–3 per cage under a 12 h light/12 h dark cycle. The animals had free access to food and water at all times except during the days when the corridor test was performed at which time access to food was restricted according to protocol (see below). All experimental procedures performed on rats were approved by the Ethical Committee for use of Laboratory Animals in the Lund-Malmö region. The second part of this study included a total of 6 *cynomolgus macaques* weighing 3.5–10 kg that were housed individually with free access to food and water. All experimentation on the monkeys was performed with approval from the Institutional Animal Care and Use Committee and Institutional Biosafety Committee at Rush University.

Neurotoxic lesions. *6-OHDA lesions in rat.* The surgical procedures were conducted under anesthesia induced by an i.p. injection of a 20 : 1 mixture of fentanyl citrate 300 mg/kg (Fentanyl, Apoteksbolaget, Sweden) and medetomidine hydrochloride (Dormitor, Apoteksbolaget, Sweden) at a dose 6 ml/kg (300 mg/kg and 0.3 mg/kg, respectively). The animal was placed in a stereotactic frame (Stoelting, Wood Dale, IL) and intracerebral injections were made with a Hamilton syringe (Hamilton, Bonaduz, Switzerland). The anteroposterior (AP) and mediolateral (ML) coordinates were calculated from bregma and the dorsoventral (DV) coordinates from the dural surface, according to the atlas of Watson and Paxinos[24]. Complete unilateral DA lesions[25] were achieved by injecting 14 μg free base 6-OHDA (Sigma-Aldrich AB, Sweden) in ascorbate-saline (0.02%), at a concentration of 3.5 μg/μl into the right medial forebrain bundle, using the following coordinates: AP: −4.4 mm; ML: −1.2 mm and DV: −7.8 mm with the tooth bar set to −2.4 mm using a 26-gauge needle attached to the Hamilton syringe. The 6-OHDA was injected at a speed of 1 μl/min and the needle was kept in place for 3 min before it was slowly retracted.

MPTP treatment in monkey. Briefly, all monkeys were put under isofluorane anesthesia and then their right carotid artery surgically were exposed, the right external carotid artery permanently ligated, and 3 mg MPTP-HCl injected into the right common carotid artery at 1.33 ml/min in the opposite direction to the blood flow [For further details see Kordower et al.[26]]. This lesion paradigm affects predominantly the ipsilateral side of the brain. Subsequently the animals were subjected to iv injections of MPTP (0.3 mg/kg) weekly until stable parkinsonian features were established bilaterally using the CRS.

AAV vectors. AAV vectors of serotype 5 were used in this study, with the transgenes flanked by inverted terminal repeats from AAV serotype 2 and packaged in an AAV serotype 5 capsid. The TH-GCH1 vector contained the human TH and GCH1 genes, each driven by a human Syn-1 promoter. The GCH1 gene was terminated by an early SV40 poly-A sequence, whereas the upstream TH gene was followed by a WPRE to improve trafficking of the TH mRNA. The full sequence was terminated by an early SV40 poly-A sequence [See Cederfjäll et al.[16] for details of the vector construct]. Two alternative versions of this vector were created as controls where the TH gene was substituted for a second copy of the GCH1 gene (GCH1-GCH1) in the rodent study or with a gene encoding GFP (GFP-GCH1) in the monkey study. The same TH-GCH1 vector preparation was used in both rodent and monkey.

The production of AAV vectors was achieved with a two plasmid transfection method where the essential adenoviral packaging genes were delivered in *trans* with a helper plasmid, as described previously[27]. The vector preparations were purified by iodixanol step gradients and Sepharose Q column chromatography[28] and then titered using TaqMan quantitative PCR[29] using primers and probes targeted towards the WPRE sequence. For the rodent dose-response study, serial dilutions were made from a single TH-GCH1 vector batch, which had a stock titer of 2.7E13 gc/ml. Highest titer group received the stock solution directly (resulting in 1.3E11 gc injected per animal), while dilutions were made to create vector solutions with titers of 2.6E12 gc/ml (resulting in 1.3E10 gc injected per animal), 9.1E11 gc/ml (resulting in 4.6E9 gc injected per animal) and 1.8E11 gc/ml (resulting in 9.1E8 gc injected per animal). The titer of the control vector (GCH1-GCH1) was matched with the full titer TH-GCH1 to 3.0E13 gc/ml (resulting in 1.5E11 gc injected per animal). For the monkey study, a TH-GCH1 vector batch with a titer of 6.6E13 gc/ml (resulting in a total of 2.6E12 gc injected per hemisphere), whereas the GFP-GCH1 vector had a titer of 5.3E13 gc/ml (resulting in a total of 2.1E12 gc injected per hemisphere).

Vector injections. *Rodent vector injections.* Animals in the vector-treatment groups received intrastriatal injections of 5 μl AAV vector suspended in ringer lactate solution, whereas animals in the intact and lesion control groups underwent sham surgery by making a burr hole at the corresponding position in the skull but without penetrating the dura. The injections were made at two sites with two deposits along the tracts, i.e. 1.5 μl in the ventral and 1.0 μl in the dorsal deposit in each injection site. The vector was delivered using a pulled glass capillary (outer diameter 60–80 μm) mounted on a 22-gauge needle attached to the Hamilton syringe. The injection coordinates were: (1) AP: +1.0 mm; ML: −2.8 mm and DV: −4.5, −3.5 mm and (2) AP: 0.0 mm; ML: −4.0 mm and DV: −5.0, −4.0 mm with the tooth bar set to −2.4 mm. The AAV vector was injected at a speed of 0.4 μl/min and the needle was kept in place for 1 min after the ventral and 3 min after the dorsal deposit was delivered, before it was slowly retracted.

Monkey vector injections. Six monkeys (TH-GCH1 n = 3, GFP-GCH1 n = 3) with stable parkinsonian symptoms received bilateral AAV vector injections targeting the caudate nucleus, anterior putamen and post-commissural putamen[26,30]. Stereotactic injections were made at two sites in the caudate (at 10 and 5 μl) and at three sites in the putamen (10, 10, 5 μl). In total 40 μl vector was injected per hemisphere at a rate of 1 μl/min. Injection coordinates were determined using an MRI based localization.

Rodent behavioral tests. *Amphetamine-induced rotation* test was performed at a single time-point four weeks after 6-OHDA lesion. This test was used to exclude animals in which the lesion was incomplete. After an injection of D-amphetamine sulfate (2.5 mg/kg, i.p., Apoteksbolaget, Sweden) full left and right body turns were quantified over 90 minutes using automated rotometer bowls (AccuScan Instruments Inc., Columbus, Ohio), and a net ipsilateral rotational asymmetry score of 6 full body turns/min was used as the cut-off value.

Corridor test was performed according to Dowd and colleagues[31]. Briefly, an investigator blinded to the group identity placed the rat in the end of a corridor (150 × 7 × 23 cm). Ten adjacent pairs of cups were evenly distanced along the floor of the corridor and each filled with 5 sugar pellets. Animals were allowed to explore the corridor freely. Retrieval of pellets was defined as each time the rat poked its nose into a unique cup, regardless of if it ate any pellets. Revisits in the same cup were not scored unless a retrieval was made from another cup in between. Each rat was tested until 20 retrievals were made or the maximum time of 5 min for the test duration elapsed. The rats were food restricted throughout testing period. Prior to the first test session, animals were habituated for 2 days á 10 minutes in the corridor with sugar pellets scattered along the floor. The rats were placed in an empty corridor for 5 minutes before testing to reduce novelty of the environment, which stabilized the performance of the animals in the test. Results were calculated as an average of the contralateral retrievals (left) and presented as percentage of total retrievals.

Stepping test, originally described by Schallert and colleagues[32], was performed in this study according to the modified side-stepping described in Olsson et al.[33]. An investigator blinded to the group identities of the animals assessed forelimb use by holding the rat with two hands only allowing one forepaw to reach the table surface. The animal was then moved sideways over a defined distance of 90 cm at a constant speed over 4–5 sec. The investigator scored the numbers of adjusting side steps in both forehand and backhand direction twice on a testing day, and the average was calculated over 3 testing days. The animals were pre-trained in the stepping test one week before AAV treatment and then re-tested at 10, 12 and 14-weeks after vector treatment. At each testing point, the animals only needed habituation for one or two days and were then scored during three consecutive testing days.

Cylinder test was performed as described by Kirik et al.[34] with minor modifications from Schallert et al.[35] to assess bias in forelimb use during exploration of novel environment. For this purpose, each rat was placed in a 20 cm in diameter glass cylinder in front of two perpendicular mirrors and filmed with digital video camera. The rat was left in the cylinder until at least 20 forelimb touches on the cylinder wall were observed. Forelimb use on the cylinder wall was scored from the recording using frame-by-frame analysis by an investigator blinded to the group identity of the animals. The paw used during each of the 20 contacts with the cylinder walls during rearing was scored and presented as percentage left forepaw touches of total wall contacts with either forepaw.

Monkey behavioral tests. A non-human primate CRS, as described by Kordower et al.[26,30], was used to quantify parkinsonian-like impairment in the MPTP-treated monkeys and was performed throughout the study by an investigator blinded to the group identities. All animals were pre-scored at four different time points before

starting MPTP treatment. Animals were followed over an 18-month period where each month contained 4 test sessions. Stable parkinsonian impairment was established in all animals after 12 months, and received AAV vector injections thereafter as described above. Animals were then further assessed for 6 months post-AAV. In addition to drug-naïve assessment, all animals were challenged with s.c. injections of L-DOPA (10, 20, 40 mg/mg with benserazide) both before and after AAV vector injection (i.e. after last time point pre-AAV and after last time point) in an effort to establish whether the dose-response characteristics to L-DOPA shifted following treatment.

Microdialysis in monkey. After the last behavioral assessment at 6 months post-AAV all vector-treated animals and two intact animals were included in a microdialysis study. Under isoflurane anesthesia, the animals received bilateral putaminal probes (modified CMA 12 with extended shaft length (24 mm) and membrane length (7 mm)) (CMA, Kista, Sweden). Artificial CSF (CMA) was used as dialysate with a CMA 402 pump at a flow rate of 4 μl/min. After passing the probe the brain dialysate was mixed with an anti-oxidant solution (1 mol/l HAc, 0.27 mmol/l EDTA, 33 mmol/l L-cysteine, and 5 mmol/l ascorbic acid[36]). One hour equilibration, five baseline samples were collected with a CMA 470 refrigerated fraction collector every 20 minutes in glass vials containing 10 μl 0.1 M perchloric acid and then immediately frozen on dry-ice. At the end of the collection of fifth baseline sample all animals received an i.v. injection of the central AADC inhibitor NSD-1015 (100 mg/kg in saline) to study in vivo TH activity. Samples were collected for two hours after NSD-1015 injection. At the end of the microdialysis session, the animals were perfused with 4% paraformaldehyde (PFA) for histological assessment, while dialysates were analyzed by high performance liquid chromatography (HPLC).

HPLC analysis of monoamines. Dialysates were analyzed by HPLC with the Alexys monoamine analyzer system (Antec Leyden, The Netherlands) consisting of a DECADE II detector and VT-3 electrochemical flow cell. Two different mobile phases, optimized for the detection of the respective metabolites, were used in each of the two parallel flow paths. The first mobile phase (50 mM phosphoric acid, 8 mM NaCl, 0.1 mM EDTA, 12.5% methanol, 500 mg/l octane sulphate; pH 6.0) was used for the detection of DA through a 1 mm × 50 mm column with 3 mm particle size (ALF-105) at a flow rate of 75 ml/min. The second mobile phase (50 mM phosphoric acid, 50 mM citric acid, 8 mM NaCl, 0.1 mM EDTA, 10% methanol, 600 mg/l octane sulphate; pH 3.2) was used for the detection of DOPA, 3-OMD, DOPAC and HVA, which passed through a 1 mm × 150 mm column with 3 mm particle size (ALF-115) at a flow rate of 100 ml/min. Peak identification and quantification was conducted using the Clarity chromatographic software package (DataApex, Prague, Czech Republic).

Histological analysis. In the rodent study, six rats from each dose of the TH-GCH1 groups, five from GCH1-GCH1 and three from Les-Sham were anaesthetized by an i.p. injection of 1.2 ml sodium pentobarbital (Apoteksbolaget, Sweden) and then transcardially perfused with 50 ml room temperature saline followed by 250 ml ice-cold 4% paraformaldehyde (PFA) in 0.1 M phosphate buffer adjusted to pH 7.4, at a 50 ml/min rate. The brains were then dissected and post-fixated in 4% PFA for 2 hours before cryoprotection in 25% sucrose for 24–48 hours. The fixed brains were cut in coronal orientation at a thickness of 35 μm on a semi-automated freezing microtome (Microm HM 450) and collected in 6 series and stored in anti-freeze solution (0.5 M sodium phosphate buffer, 30% glycerol and 30% ethylene glycol) at −20°C until further processing. Immunohistochemistry was performed using antibodies raised against TH (P40101-0, rabbit IgG 1 : 2000 Pel-Freez, Rogers, AR), GCH1 (MCA3138Z, mouse IgG 1 : 2000 AbD Serotec, Oxford, UK), AADC (AB1569, rabbit IgG, 1 : 500, Millipore, Billerica, MA), NeuN (MAB377, mouse IgG 1 : 500, Millipore), IBA1 (019-19741, rabbit IgG 1 : 1000, Wako, Richmond, VA), and ED1 (MCA341-R, mouse IgG 1 : 200, Serotec, Oxford, UK). Incubation with biotinylated secondary antibodies (BA1000, goat anti-rabbit and BA2001, horse anti-mouse, Vector Laboratories, Burlingame, CA) was followed by a second 1-hour incubation with avidin-biotin peroxidase solution (ABC Elite, Vector Laboratories, Burlingame, CA). The staining was visualized using 3,3′-diaminobenzidine in 0.01% H$_2$O$_2$.

Perfusion and histological processing in monkey. Monkeys were anaesthetized with ketamine (15 mg/kg, i.m.), anesthetized with pentobarbital (25 mg/kg, i.v.), intubated and then perfused with warm followed by ice-cold saline followed by fixation with 4% PFA. Once removed from the calvaria, brains were placed in 30% sucrose/PBS until fully immersed. Sections were cut frozen on a sliding knife microtome at a 40 μm thickness and stored in cryoprotectant.

Stereological analysis. In the rat study, NeuN, GCH1 and TH-positive cells in striatum and GP were quantified with design-based stereology utilizing the areal counting frame originally described by Gundersen[37]. A Nikon Eclipse 80i light microscope connected to the NewCast Module in VIS software (*Visiopharm A/S*, Horsholm, Denmark) was used. Striatum and GP were delineated unilaterally in 2 × magnification in the entire rostrocaudal axis, approximately between bregma 2.28 mm and −2.76 mm and bregma −0.24 mm and −2.76 mm for striatum and GP respectively[24]. Every 16th section was quantified for striatal counts, resulting in 7–8 sections per brain. For the globus pallidus every 8th section was quantified (8–10 sections/brain). Quantification was performed with a 60x Plan-Apo oil lens (NA = 1.4) by a researcher blinded to the group identity of the animals. The fraction settings were adjusted so at least 150 cells were counted for each brain region. The optical

fractionator principle was then used to estimate the total number of objects present in the target nuclei[38]. In the monkey study, every other GCH1 and NeuN stained section of striatum and caudate nucleus was bilaterally quantified using a modification of the schema described above.

Statistical analysis. Statistical comparisons between groups and over time were conducted with the SPSS statistical package (SPSS Inc., Chicago, IL). The data presented in figure 2 was first analyzed with a repeated measures ANOVA using the general linear model followed by one-way ANOVAs at each time point and Tukey's HSD when Levene's test was significant (P < 0.05), otherwise Dunnett's T3 test was used. For data presented in figure 6, one-way ANOVA tests were followed by *post hoc* comparison with Tukey's HSD or Dunnett's T3 test.

1. Fahn, S. Parkinson disease, the effect of levodopa, and the ELLDOPA trial. Earlier vs Later L-DOPA. *Arch Neurol* **56**, 529–535 (1999).
2. Nutt, J. G. & Holford, N. H. The response to levodopa in Parkinson's disease: imposing pharmacological law and order. *Ann Neurol* **39**, 561–573 (1996).
3. Obeso, J. A., Olanow, C. W. & Nutt, J. G. Levodopa motor complications in Parkinson's disease. *Trends Neurosci* **23**, S2–7 (2000).
4. Kurlan, R. *et al.* Duodenal delivery of levodopa for on-off fluctuations in parkinsonism: preliminary observations. *Ann Neurol* **20**, 262–265 (1986).
5. Nilsson, D. *et al.* Long-term intraduodenal infusion of a water based levodopa-carbidopa dispersion in very advanced Parkinson's disease. *Acta Neurol Scand* **97**, 175–183 (1998).
6. Sage, J. I., Trooskin, S., Sonsalla, P. K., Heikkila, R. & Duvoisin, R. C. Long-term duodenal infusion of levodopa for motor fluctuations in parkinsonism. *Ann Neurol* **24**, 87–89 (1988).
7. Stocchi, F., Vacca, L., Ruggieri, S. & Olanow, C. W. Intermittent vs continuous levodopa administration in patients with advanced Parkinson disease: a clinical and pharmacokinetic study. *Arch Neurol* **62**, 905–910 (2005).
8. Bjorklund, T., Carlsson, T., Cederfjall, E. A., Carta, M. & Kirik, D. Optimized adeno-associated viral vector-mediated striatal DOPA delivery restores sensorimotor function and prevents dyskinesias in a model of advanced Parkinson's disease. *Brain* **133**, 496–511 (2010).
9. Carlsson, T. *et al.* Reversal of dyskinesias in an animal model of Parkinson's disease by continuous L-DOPA delivery using rAAV vectors. *Brain* **128**, 559–569 (2005).
10. Corti, O. *et al.* Long-term doxycycline-controlled expression of human tyrosine hydroxylase after direct adenovirus-mediated gene transfer to a rat model of Parkinson's disease. *Proc Natl Acad Sci U S A* **96**, 12120–12125 (1999).
11. Kirik, D. *et al.* Reversal of motor impairments in parkinsonian rats by continuous intrastriatal delivery of L-dopa using rAAV-mediated gene transfer. *Proc Natl Acad Sci U S A* **99**, 4708–4713 (2002).
12. Mandel, R. J. *et al.* Characterization of intrastriatal recombinant adeno-associated virus-mediated gene transfer of human tyrosine hydroxylase and human GTP-cyclohydrolase I in a rat model of Parkinson's disease. *J Neurosci* **18**, 4271–4284 (1998).
13. Szczypka, M. S. *et al.* Viral gene delivery selectively restores feeding and prevents lethality of dopamine-deficient mice. *Neuron* **22**, 167–178 (1999).
14. Muramatsu, S. *et al.* Behavioral recovery in a primate model of Parkinson's disease by triple transduction of striatal cells with adeno-associated viral vectors expressing dopamine-synthesizing enzymes. *Hum Gene Ther* **13**, 345–354 (2002).
15. Shen, Y. *et al.* Triple transduction with adeno-associated virus vectors expressing tyrosine hydroxylase, aromatic-L-amino-acid decarboxylase, and GTP cyclohydrolase I for gene therapy of Parkinson's disease. *Hum Gene Ther* **11**, 1509–1519 (2000).
16. Cederfjall, E., Sahin, G., Kirik, D. & Bjorklund, T. Design of a single AAV vector for coexpression of TH and GCH1 to establish continuous DOPA synthesis in a rat model of Parkinson's disease. *Mol Ther* **20**, 1315–1326 (2012).
17. Alexander, T., Sortwell, C. E., Sladek, C. D., Roth, R. H. & Steece-Collier, K. Comparison of neurotoxicity following repeated administration of l-dopa, d-dopa and dopamine to embryonic mesencephalic dopamine neurons in cultures derived from Fisher 344 and Sprague-Dawley donors. *Cell Transplant* **6**, 309–315 (1997).
18. Chen, L. *et al.* Unregulated cytosolic dopamine causes neurodegeneration associated with oxidative stress in mice. *J Neurosci* **28**, 425–433 (2008).
19. Cheng, N. *et al.* Differential neurotoxicity induced by L-DOPA and dopamine in cultured striatal neurons. *Brain Res* **743**, 278–283 (1996).
20. Ciesielska, A. *et al.* Cerebral infusion of AAV9 vector-encoding non-self proteins can elicit cell-mediated immune responses. *Mol Ther* **21**, 158–166 (2013).
21. Bankiewicz, K. S. *et al.* Convection-enhanced delivery of AAV vector in parkinsonian monkeys; in vivo detection of gene expression and restoration of dopaminergic function using pro-drug approach. *Exp Neurol* **164**, 2–14 (2000).
22. Bankiewicz, K. S. *et al.* Long-term clinical improvement in MPTP-lesioned primates after gene therapy with AAV-hAADC. *Mol Ther* **14**, 564–570 (2006).
23. Dodiya, H. B. *et al.* Differential transduction following basal ganglia administration of distinct pseudotyped AAV capsid serotypes in nonhuman primates. *Mol Ther* **18**, 579–587 (2010).
24. Watson, C. & Paxinos, G. The Rat Brain in Stereotaxic Coordinates. *Academic Press: San Diego, CA.* (1986).

25. Ungerstedt, U. & Arbuthnott, G. W. Quantitative recording of rotational behavior in rats after 6-hydroxy-dopamine lesions of the nigrostriatal dopamine system. *Brain Res* **24**, 485–493 (1970).

26. Kordower, J. H. *et al.* Neurodegeneration prevented by lentiviral vector delivery of GDNF in primate models of Parkinson's disease. *Science* **290**, 767–773 (2000).

27. Ulusoy, A., Sahin, G., Bjorklund, T., Aebischer, P. & Kirik, D. Dose optimization for long-term rAAV-mediated RNA interference in the nigrostriatal projection neurons. *Mol Ther* **17**, 1574–1584 (2009).

28. Zolotukhin, S. *et al.* Production and purification of serotype 1, 2, and 5 recombinant adeno-associated viral vectors. *Methods* **28**, 158–167 (2002).

29. Zolotukhin, S. *et al.* Recombinant adeno-associated virus purification using novel methods improves infectious titer and yield. *Gene Ther* **6**, 973–985 (1999).

30. Kordower, J. H. *et al.* Delivery of neurturin by AAV2 (CERE-120)-mediated gene transfer provides structural and functional neuroprotection and neurorestoration in MPTP-treated monkeys. *Ann Neurol* **60**, 706–715 (2006).

31. Dowd, E., Monville, C., Torres, E. M. & Dunnett, S. B. The Corridor Task: a simple test of lateralised response selection sensitive to unilateral dopamine deafferentation and graft-derived dopamine replacement in the striatum. *Brain Res Bull* **68**, 24–30 (2005).

32. Schallert, T., De Ryck, M., Whishaw, I. Q., Ramirez, V. D. & Teitelbaum, P. Excessive bracing reactions and their control by atropine and L-DOPA in an animal analog of Parkinsonism. *Exp Neurol* **64**, 33–43 (1979).

33. Olsson, M., Nikkhah, G., Bentlage, C. & Bjorklund, A. Forelimb akinesia in the rat Parkinson model: differential effects of dopamine agonists and nigral transplants as assessed by a new stepping test. *J Neurosci* **15**, 3863–3875 (1995).

34. Kirik, D., Georgievska, B., Rosenblad, C. & Bjorklund, A. Delayed infusion of GDNF promotes recovery of motor function in the partial lesion model of Parkinson's disease. *Eur J Neurosci* **13**, 1589–1599 (2001).

35. Schallert, T., Fleming, S. M., Leasure, J. L., Tillerson, J. L. & Bland, S. T. CNS plasticity and assessment of forelimb sensorimotor outcome in unilateral rat models of stroke, cortical ablation, parkinsonism and spinal cord injury. *Neuropharmacology* **39**, 777–787 (2000).

36. Thorre, K., Pravda, M., Sarre, S., Ebinger, G. & Michotte, Y. New antioxidant mixture for long term stability of serotonin, dopamine and their metabolites in automated microbore liquid chromatography with dual electrochemical detection. *J Chromatogr B Biomed Sci Appl* **694**, 297–303 (1997).

37. Gundersen, H. J. & Jensen, E. B. The efficiency of systematic sampling in stereology and its prediction. *J Microsc* **147**, 229–263 (1987).

38. West, M. J. Stereological methods for estimating the total number of neurons and synapses: issues of precision and bias. *Trends Neurosci* **22**, 51–61 (1999).

Author contributions

E.C. performed the study. T.B. participated in post-mortem analysis. N.N. performed the rodent stereology. The non-human primate experiment was carried out in the lab of JHK. E.C., G.S. and D.K. did microdialysis in non-human primates. Y.C. performed confocal analysis and E.N. carried out the non-human primate stereology. D.K. and J.H.K. supervised the project. E.C., J.H.K. and D.K. prepared the manuscript and all authors reviewed it.

Additional information

Competing financial interests: DK and TB are co-inventors of a patent application on the construct reported in this paper. TB is a founding-director of a company that intends to develop this for commercial purposes. DK receives financial compensation in the form of retainer fees, milestones and royalty payments. JHK is a Founding Scientist and currently an SAB member of Ceregene Inc. EC, NN, GS, EN and YC have no conflict of interest.

How to cite this article: Cederfjäll, E. *et al.* Continuous DOPA synthesis from a single AAV: dosing and efficacy in models of Parkinson's disease. *Sci. Rep.* **3**, 2157; DOI:10.1038/srep02157 (2013).